

## Supporting Information

### **Flexible and adhesive liquid-free ionic conductive elastomers toward human-machine interaction**

*Zhenyu Xu,<sup>a,b</sup> Rui Li,<sup>a</sup> Huijing Li,<sup>a,b</sup> Guorong Gao<sup>\*a,b</sup> and Tao Chen<sup>\*a,b</sup>*

<sup>a</sup> Key Laboratory of Marine Materials and Related Technologies, Zhejiang Key Laboratory of Marine Materials and Protective Technologies, Ningbo Institute of Materials Technology and Engineering, Chinese Academy of Sciences, Ningbo 315201, China. E-mail: gaogr@nimte.ac.cn, tao.chen@nimte.ac.cn

<sup>b</sup> School of Chemical Sciences, University of Chinese Academy of Sciences, Beijing 100049, China

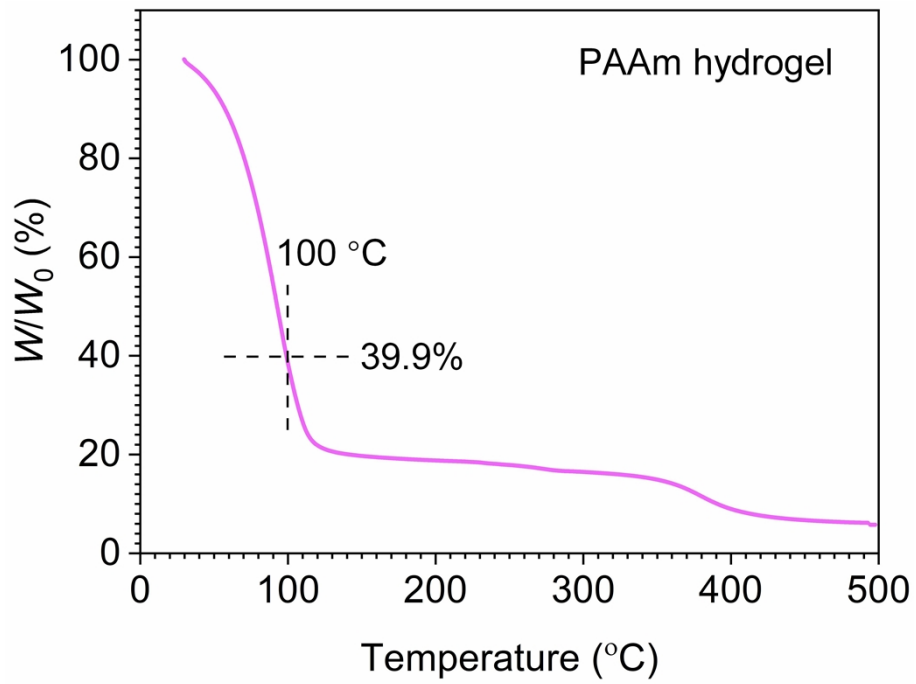


**Fig. S1** TGA curve of a PAAm hydrogel.

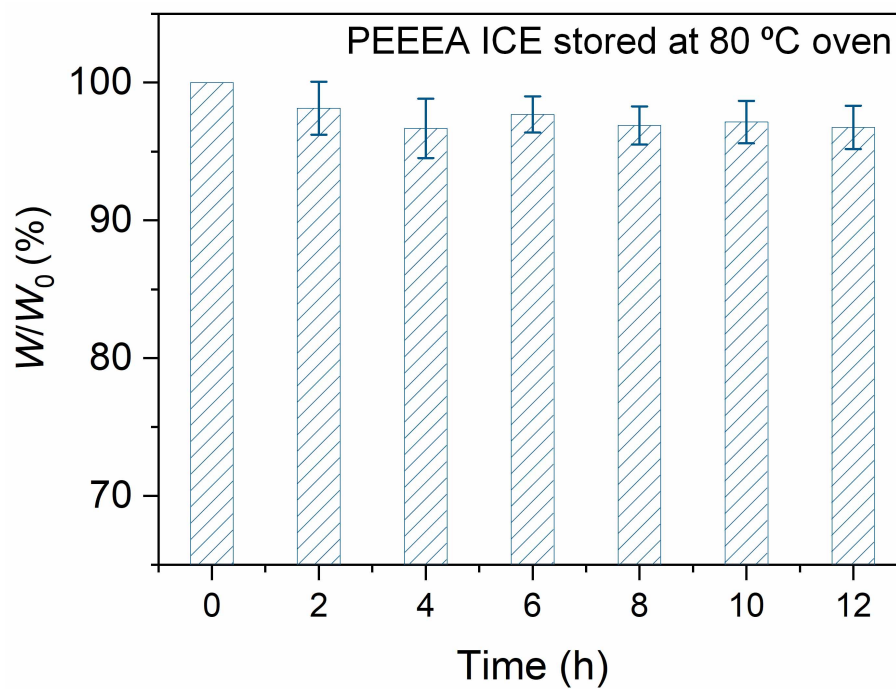


**Fig. S2** Weight retention rate changed by time as the PEEEA ICE stored in an oven at 80 °C.

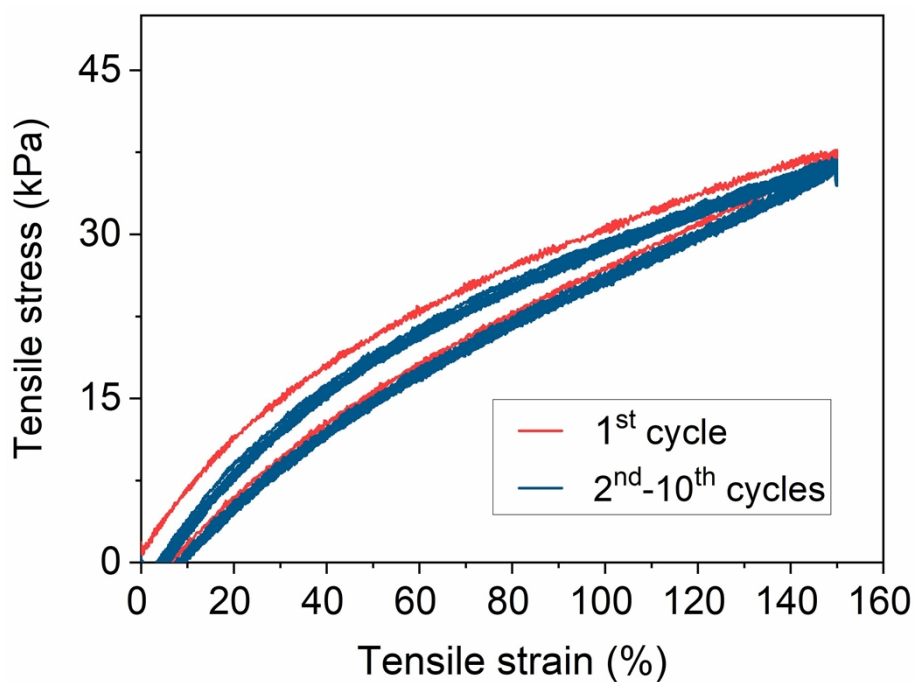


**Fig. S3** Cyclic tensile stress-strain curves of an ICE.

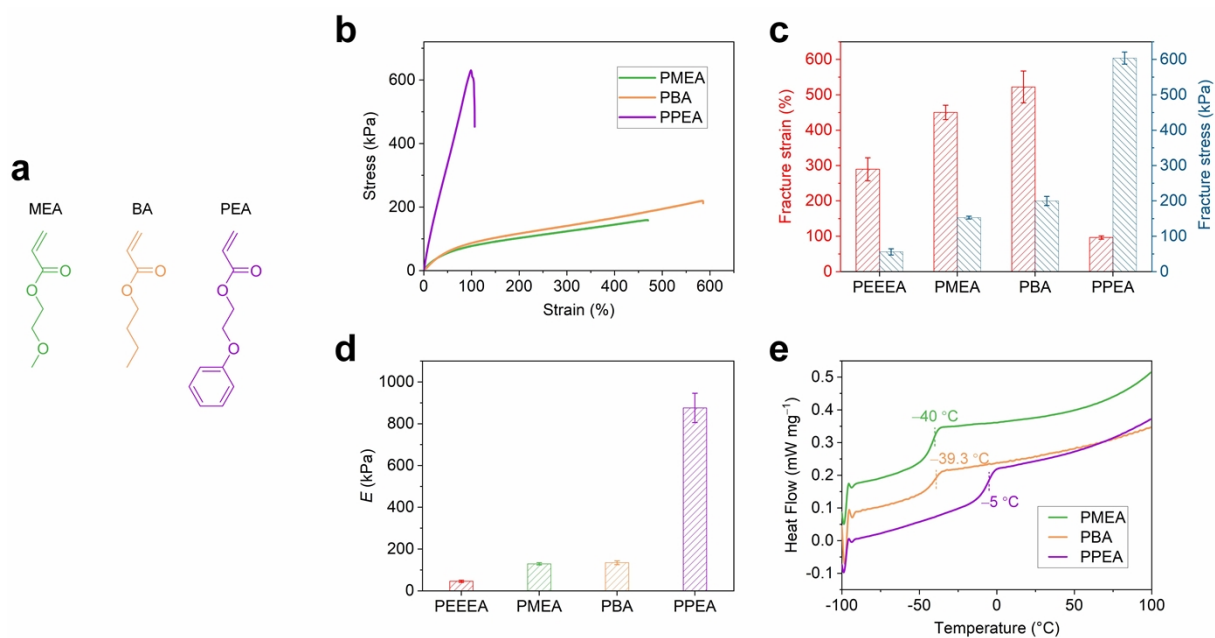


**Fig. S4** (a) Molecular structure of MEA, BA, and PEA. (b) Typical tensile stress-strain curves, (c) the summarized fracture strain and fracture stress, (d) initial modulus ( $E$ ), and (e) typical DSC curves of PME ICE, PBA ICE, and PPE ICE.

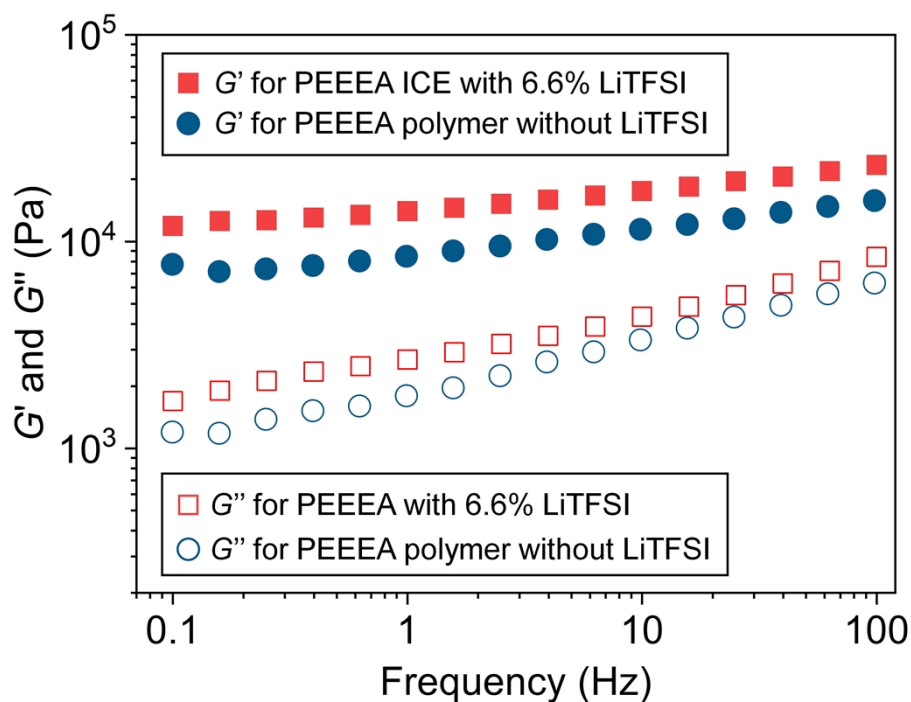


**Fig. S5** Storage modulus ( $G'$ ) and loss modulus ( $G''$ ) changed by frequency for PEEEA polymer without LiTFSI and PEEEA ICE with 0.5% LiTFSI in rheological tests.

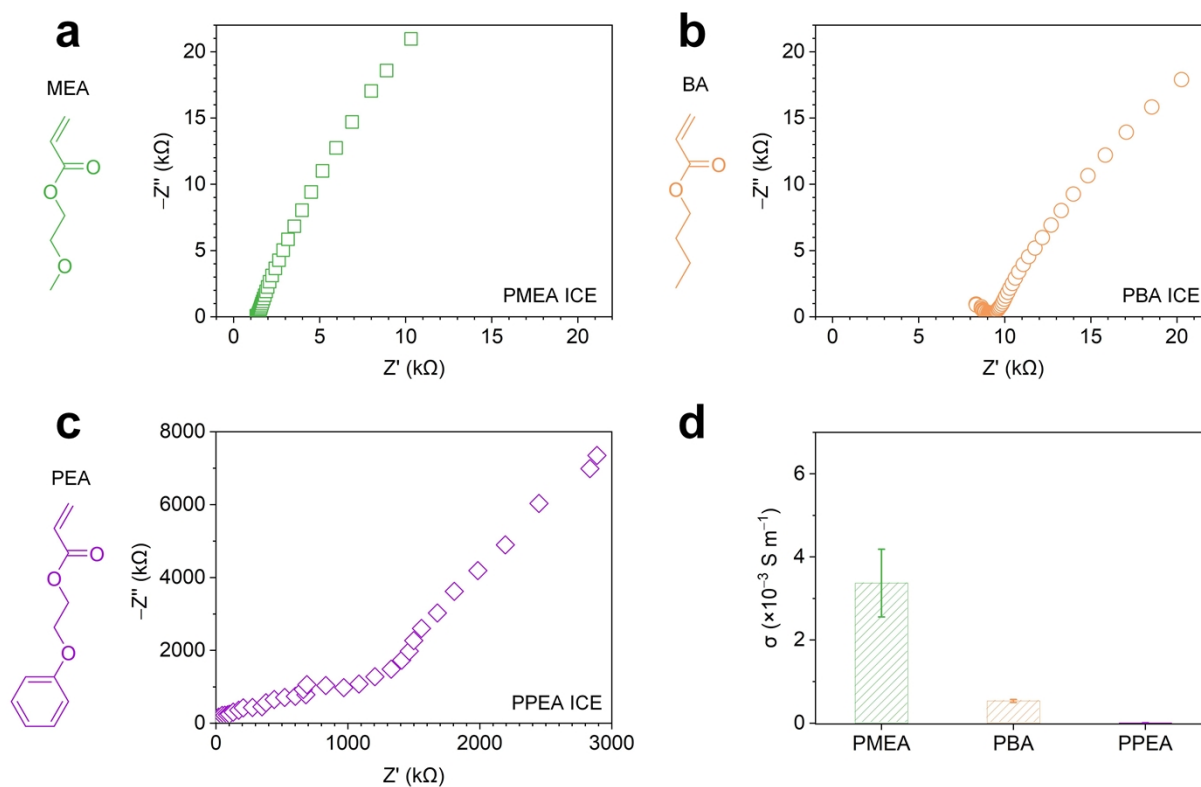


**Fig. S6** (a) Typical Nyquist plots of PMEa ICE, PBA ICE, and PPEA ICE. (d) The summarized conductivity ( $\sigma$ ) of PMEa ICE, PBA ICE, and PPEA ICE.

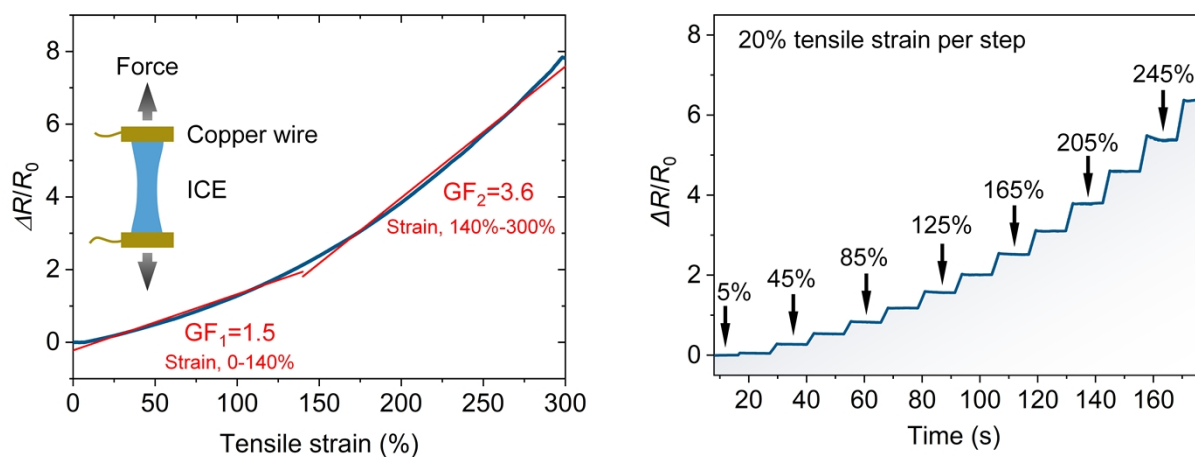


**Fig. S7** The relative resistances ( $\Delta R/R_0$ ) changed by stretching (left) and gradually stretching (right) with an increment of 20% strain at each step. The gauge factor (GF) is labelled on the left curve.

**Movie S1** Tapping the TENG on the hand to enter letters.

**Movie S2** Tapping the TENG adhered to the electrical shell to enter letters.